

1
2
3
4
5
6
7
8
9
10

Immunoinformatics approach identified two highly conserved B and T cell epitopes, LEASKRWAF and DSPLEASKRWAFRTG, for effective vaccine design against Ebola and Marburg Viruses

ABSTRACT

Aims: Ebola and Marburg viruses cause fatal hemorrhagic fever in both human and non-human primates. Absence of any licensed vaccine has further deteriorated the problem. In the present study, we aimed to design potential epitope based vaccines against these viruses using computational approaches.

Methodology: By using various bioinformatics tools and databases, we analyzed the conserved glycoprotein sequences of Ebola and Marburg viruses and predicted two potential epitopes which may be used as peptide vaccines.

Results: Using various B-cell and T-cell epitope prediction servers, four highly conserved epitopes were identified. Epitope conservancy analysis showed that “LEASKRWAF” and “DSPLEASKRWAFRTG” epitopes were 100% and 93.62% conserved and the worldwide population coverage of “LEASKRWAF” interacting with MHC class I molecules and “DSPLEASKRWAFRTG” interacting with MHC class II molecules were 78.74% and 75.75% respectively. Immunoinformatics analysis showed that they are highly immunogenic, flexible and accessible to antibody. Molecular docking simulation analysis demonstrated a very significant interaction between epitopes and MHC molecules with lower binding energy. Cytotoxic analysis and ADMET test also supported their potential as vaccine candidates.

Conclusion: In sum, our in silico approach demonstrated that both “LEASKRWAF” and “DSPLEASKRWAFRTG” hold the promise for the development of common vaccine against Ebola and Marburg viruses.

Keywords: B cell; T cell; Vaccine; Epitope; Ebola and Marburg viruses

Abbreviations: EBOV (Ebola virus); MARV (Marburg virus); GP (glycoprotein)

1. INTRODUCTION

Ebola virus (EBOV) and Marburg virus (MARV), belong to the family Filoviridae (filoviruses), are among the deadliest human pathogenic viruses which cause the outbreak of viral hemorrhagic fever in Africa with high fatality rate [1, 2]. These viruses can be transmitted between humans and from non-human hosts through contact with infectious bodily fluids [3, 4]. Their natural reservoirs are fruit bats, predominantly the Egyptian fruit bat (*Rousettus aegyptiacus*), which makes its transmission particularly dangerous [5]. Both viruses are classified as category A pathogens with no licensed vaccine or treatment available for human use and are handled in maximum containment laboratories [2]. The genus Ebolavirus is composed of five species such as, Bundibugyo virus (BDBV; species Bundibugyo ebolavirus); Ebola virus (EBOV; species Zaire ebolavirus); Sudan virus (SUDV; species Sudan ebolavirus); Tai Forest virus (TAFV; species Tai Forest ebolavirus) and Reston virus (RESTV; species Reston ebolavirus), with the newly discovered currently unclassified Bombali virus (BOMV; species Bombali ebolavirus) [6]. In contrast, the genus Marburgvirus has only one species, the Marburg marburgvirus, with two known strains Marburg virus (MARV) and Ravn virus (RAVV), which has approximately 20% divergent at the amino acid level [2].

11

12

13

14

15

16

17

18

19

20

21

22

23

24

25

26

27

28

29

30 Filoviruses are filamentous in appearance and have non-segmented single strand negative sense RNA genome which is
31 approximately 19 kb in length [7]. The viral RNA genome encode seven proteins which are translated from a single
32 monocistronic mRNA, such as nucleoprotein [8], major (VP40) and minor (VP24) matrix proteins, RNA-dependent RNA
33 polymerase (L), polymerase cofactor (VP35), transcription activator (VP30), and a glycoprotein (GP) [9, 10]. The genome
34 is tightly associated with the nucleoprotein [8] and viral protein 30 (VP30), which along with viral protein 35 (VP35) and the
35 L-polymerase (L) protein form the central nucleocapsid core [10]. The nucleocapsid core is surrounded by a matrix,
36 comprising viral protein 40 (VP40) and viral protein 24 (VP24) and a host-derived lipid envelope composed of anchored
37 glycoprotein (GP) [7]. The MARV VP40 has been known to inhibit protein tyrosine phosphorylation of STAT thereby
38 blocking the Jak-STAT pathway. On the other hand, EBOV VP24 obstructs the interferon induced pathway by preventing
39 nuclear accumulation of phosphorylated STAT1 [11, 12]. VP35 is another protein that impedes interferon production by
40 inhibiting retinoic-acid inducible gene-I (RIG-I)-like receptor (RLR) activity [13, 14]. However, GP is the most promising as
41 it protrudes outward as 7 to 10 nM spikes. Filovirus GP is involved in cell selection and entry by promoting receptor
42 binding and membrane fusion [15, 16] and has the most immunogenic potential, therefore, serves as a possible vaccine
43 candidate [17, 18].
44

45 The lethal consequences of Filoviruses become more terrifying due to the absence of any approved vaccine or drug either
46 to induce protective immunity or to control viral infection. Small inhibitor molecules have been developed to inhibit viral
47 entry, but further testing proved the method ineffective in deterring the diseases [19]. The rVSV-ZEBOV vaccine against
48 EBOV was developed in 2003, and was first used in 2016 to immunize patients [20, 21]. The vaccine was successful in
49 some cases, but it exhibited adverse effects in half of the patients, and reports of its 100% efficacy were unsupportable
50 [22]. The passive administration of monoclonal antibodies (mAbs) appeared as a promising treatment option during 2013
51 to 2016 Western African epidemic [23-28]. Although several monoclonal antibodies based vaccination strategy has been
52 developed recently and undergone clinical study, they are limited to single member of the Ebola virus genus [29, 30].
53 Recently, several human neutralizing mAb based cocktail immunotherapy has been developed which provide broad
54 protection [31-33]. Another study found complete protection against Ebola and Marburg viruses in two strains of mice
55 using T-cell epigraph vaccine [34]. So far, no universal vaccine has been licensed which can provide protection against all
56 Filoviruses irrespective of their genetic variations.
57

58 Nowadays, epitope based vaccine design against lethal viruses through bioinformatics has become popular because of its
59 short study time, increased strength to predict effective epitopes and the availability of ample sequence data. This
60 approach has been validated in various studies to fight diseases such as malaria, human immunodeficiency virus,
61 tuberculosis etc. Conserved epitope prediction by computational biology approaches not only save time, but also reduces
62 the cost associated with the vaccine development process. In the current study, we used various bioinformatics tools to
63 select peptides with high level of conservation and mapped the evolutionary conserved epitopes for entire Filovirus family.
64 We have predicted a potential conserved epitope candidate which may be used to immunize patients against both Ebola
65 and Marburg viruses.
66

67 2. MATERIAL AND METHODS

68

69 The flow chart showing graphical outline of the approaches used for peptide based vaccine design against Ebola and
70 Marburg virus has been depicted in Figure 1.



Figure 1. Graphical outline of the peptide based vaccine design against Ebola and Marburg virus.

2.1. Sequence retrieval and conserved region identification

A total of 47 glycoprotein (GP) sequences of both Marburg virus (30) and Ebola virus (17) were retrieved from UniProtKB database and downloaded in FASTA format. The length of the glycoprotein sequence was 681 amino acids. Mega 7.0 tool was used to determine the conserved sequences through multiple sequence alignment with MUSCLE algorithm, and the results were verified with Jalview [35-37].

2.2. Variability analysis of the glycoprotein

80 The conserved sequences were fed into the Protein Variability Server (PVS) to determine the absolute site variability
81 using Shannon entropy analysis [38]. Several other variability measures were also computed to calculate the absolute
82 variation in the alignment.

83 **2.3. Transmembrane topology analysis and glycosylation site prediction**

84 As the epitopes need to be in the exposed regions of the protein to yield the best response, they were analyzed using
85 TMHMM v2.0 server to identify the inner, outer and transmembrane helix regions [39]. The protein was then analyzed to
86 identify the glycosylation sites using NetOGlyc 4.0 Server, and the results were verified using NetNGlyc 1.0 Server [40,
87 41]. The epitopes without glycosylation sites were used in further analyses.

88 **2.4. Prediction of antigenicity**

89 Antigenicity determines the success of a subunit vaccine by inducing an immune response and providing protection from
90 future infections. The conserved sequence was tested using VaxiJen v2.0 server [42], which calculates antigenicity based
91 on physiochemical properties of the protein and is not dependent on sequence alignment.

92 **2.5. Identification of the B cell epitope**

93 B lymphocytes recognize B cell epitopes on viral surface proteins and mount immune response through the differentiation
94 of plasma and memory cells. IEDB provides different methods to predict linear epitopes from protein sequences using
95 amino acid scales and Hidden Markov Models (HMM) [43]. Bepipred Linear Epitope Prediction, Chou & Fasman Beta-
96 Turn Prediction, Emini Surface Accessibility Prediction, Karplus & Schulz Flexibility Prediction, Kolaskar & Tongaonkar
97 Angenicity, Parker Hydrophilicity Prediction tools were used to predict the B cell epitopes, and the results were cross-
98 referenced with each other to obtain epitopes that fulfilled all the criteria of a highly immunogenic peptide vaccine and
99 finally verified with ABCpred server [44-48].

100 **2.6. Prediction of epitope conservancy**

101 Prediction of epitope conservancy is important to determine the effectiveness of the vaccine among population. IEDB
102 based epitope conservancy analysis tool was used to calculate the ratio of protein sequences having the epitope at a
103 given identity level [43]. Sequence identity threshold was set at least 80% for calculating the conservancy score.

104 **2.7. Prediction of population coverage**

105 Population coverage is a tool used to calculate the ratio of individual, which can mount immune response to a set of
106 epitopes with fixed MHC molecules. Allelic frequency of the interacting HLA alleles was exploited to predict the population
107 coverage for each epitope [49].

108 **2.8. Identification of T cell epitope and their interaction to MHC class I and MHC class II molecules**

109 T cell epitope is expressed on antigen presenting cell bound with Major Histocompatibility Complex (MHC) to initiate T cell
110 immune response. IEDB analysis resource provides several tools to predict T cell epitope [50-52]. T cell epitopes were
111 identified by NetCTL prediction method which predicts epitopes based on proteosomal processing, TAP transport and
112 MHC binding affinity. Artificial Neural Network (ANN) method was used to determine the half-maximal inhibitory
113 concentration (IC50) values [53, 54]. All the alleles from this site with some extra alleles relevant to this study from
114 external source were used for binding analysis. The length of the peptide was set at 9.0 to predict the epitope with MHC I
115 molecule. T cell epitopes binding to MHC class II molecules were also identified using combinatorial library, SMMalign
116 (Stabilized matrix method) and Sturniolo methods to obtain IC50 values [55].

117 **2.9. Prediction of 3-D structure and Molecular Docking Analysis of HLA and epitopes**

118 The docking analysis was performed using pdb files for HLA obtained from RCSB PDB and pdb files for the epitopes
119 created using PEP-FOLD3 server [56]. The HLA pdb files extracted from RCSB PDB were prepared by removing all
120 unnecessary molecules, adding polar hydrogens and Kollman charges. AutoDock Vina was then used to carry out the
121 docking analysis with 1.00 Å spacing and exhaustiveness = 8 [57]. The output files were then viewed with AutoDock
122 Tools and the conformation with the highest binding affinity at the correct binding site was selected. The non-bond
123 interactions (H-bonds) were then observed between the ligand and the H-bond surface of the receptor in BIOVIA
124 Discovery Studio Visualizer v17 [58].

125 **2.10. ADMET assessment of target peptides**

126 Peptide based subunit vaccine development is promising, but toxicity of the peptide epitopes interferes the success of
127 peptide based therapy. The ADMET profile of the target peptides was determined using the SwissADME tool and the
128 results were verified using admetSAR server [59, 60].

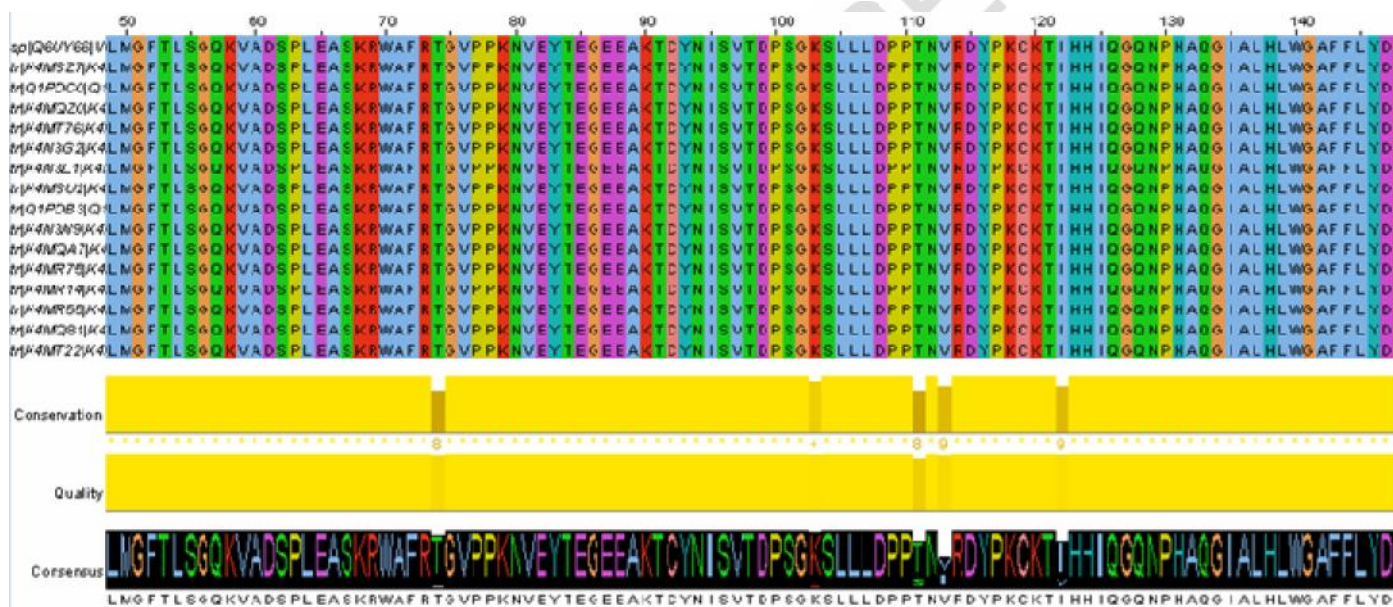
129 **2.11. Validation of the workflow**

130 The entire study was dependent on computational analyses that needed to be verified before a stable conclusion was
131 drawn. The entire workflow was put to the test by using a negative and a positive control. For the negative control, a
132 random 681 amino acid sequence was analyzed using the workflow. In contrast, for the positive control, six linear B-cell
133 epitopes of VP1 protein of coxsackievirus A16 were tested using the protein sequence extracted from NCBI [61].
134

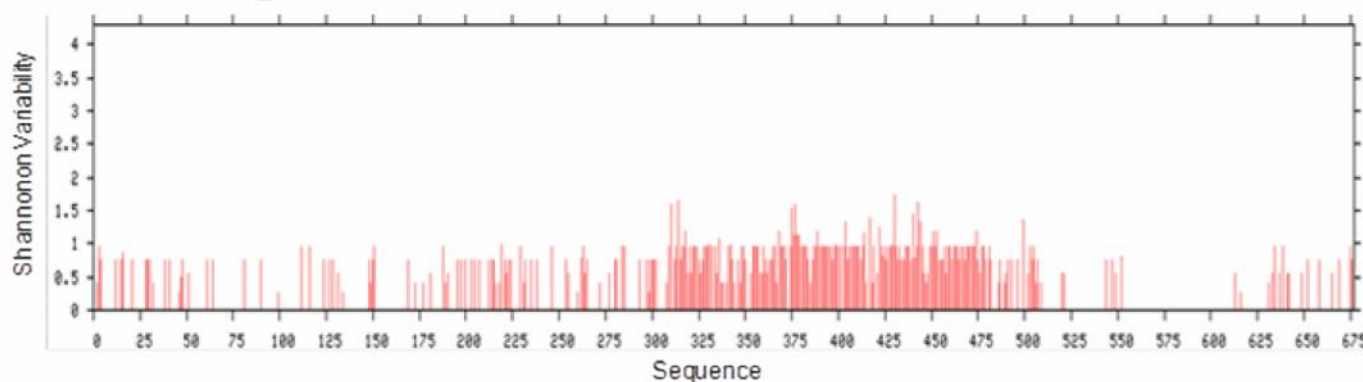
135 **3. RESULTS AND DISCUSSION**

136 **3.1. The envelope glycoprotein is highly conserved in both Ebola and Marburg viruses**

137 The degree of conservancy of specific proteins among various strains or species provides important information about its
138 evolutionary history, structure, function, and immunological properties. To determine the degree of conservation, the
139 retrieved sequences were aligned properly and an MSA was carried out with MUSCLE. MSA analysis by MUSCLE
140 revealed that envelope glycoprotein is well conserved in all sequences and the absolute variability computed by PVS
141 suggested 8 highly conserved regions (Figure 2a, 2b and Table 1). These regions were therefore selected for further
142 analysis.
143
144



145 **Figure 2.a.** Multiple sequence alignment of the retrieved sequences in Jalview. Highly conserved regions are presented
146 as shaded colors.
147
148



150
151
152
153
154
155
156

Figure 2.b. Protein variability index of G protein determined by PVS server. The conservancy threshold was 1.0 in this analysis. X axis indicates the amino acid position in sequences and Y axis indicates the Shannon entropy.

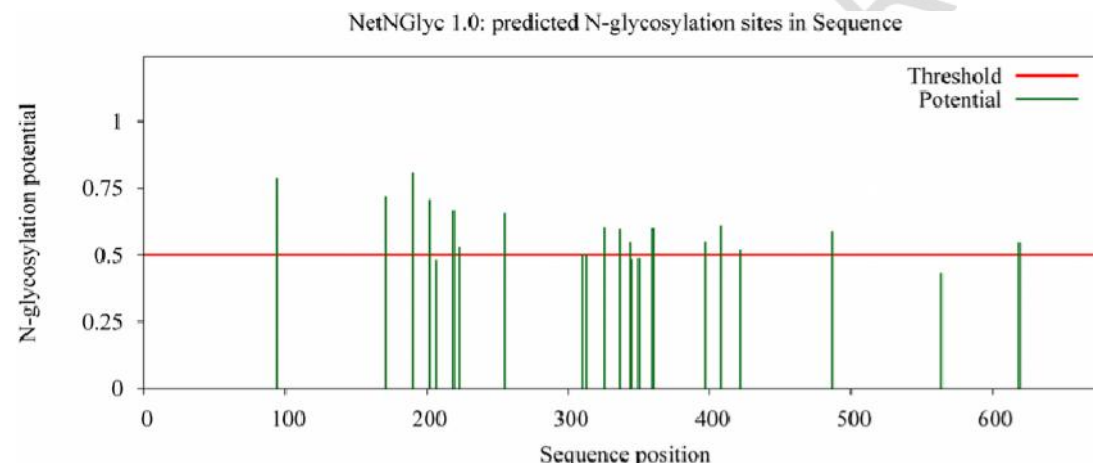
Table 1. Transmembrane topology of GP protein analyzed using THMM 2.0 server.

Conserved Regions	Topology
34-73	Outer membrane
75-102	Outer membrane
104-121	Outer membrane
123-157	Outer membrane
159-200	Outer membrane
511-546	Outer membrane
548-595	Outer membrane
597-649	Outer membrane

157
158
159
160
161
162
163
164
165

3.2. The envelope glycoprotein is highly antigenic and has large extracellular stretches

A protein must be antigenic enough to provoke sufficient immune response to be a vaccine candidate. Evaluation of the envelope glycoprotein by the VaxiJen v2.0 server suggested it as a probable antigen with the prediction value of 0.5453. A very large region of the protein (1-649) was purely on the outer membrane, while only two small segments were on the inner membrane (650-672) and transmembrane helix (673-681). The conserved regions were cross-referenced to obtain short stretches that were on the outer membrane (Table 1). The glycosylated regions were excluded from further analysis (Figure 3.).



166
167
168
169
170
171
172
173
174
175
176
177
178

Figure 3. The N-glycosylation sites of GP protein identified using NetNGlyc 1.0 server.

3.3. The highly antigenic B cell epitopes are flexible, hydrophilic and surface accessible

Several B cell epitope prediction software packages are currently used for B cell epitope prediction. Each software provides its own dataset and exploits a specific method for epitope prediction. Hence the predicted epitopes for a given protein differ from one software to another [62, 63], accurate identification of immunogenic regions in a given antigen is complicated, and prediction of false positive epitopes is a common problem [64]. Therefore, we utilized six different software packages for the B cell epitope prediction. ABCpred identified 66 16-mer epitopes with score higher than 0.5. These epitopes were cross-referenced with the results of IEDB linear B cell epitope prediction. The epitopes with higher surface accessibility scores, flexibility scores, hydrophilicity scores, and antigenicity scores were then selected (Figure 4 and Table 2).

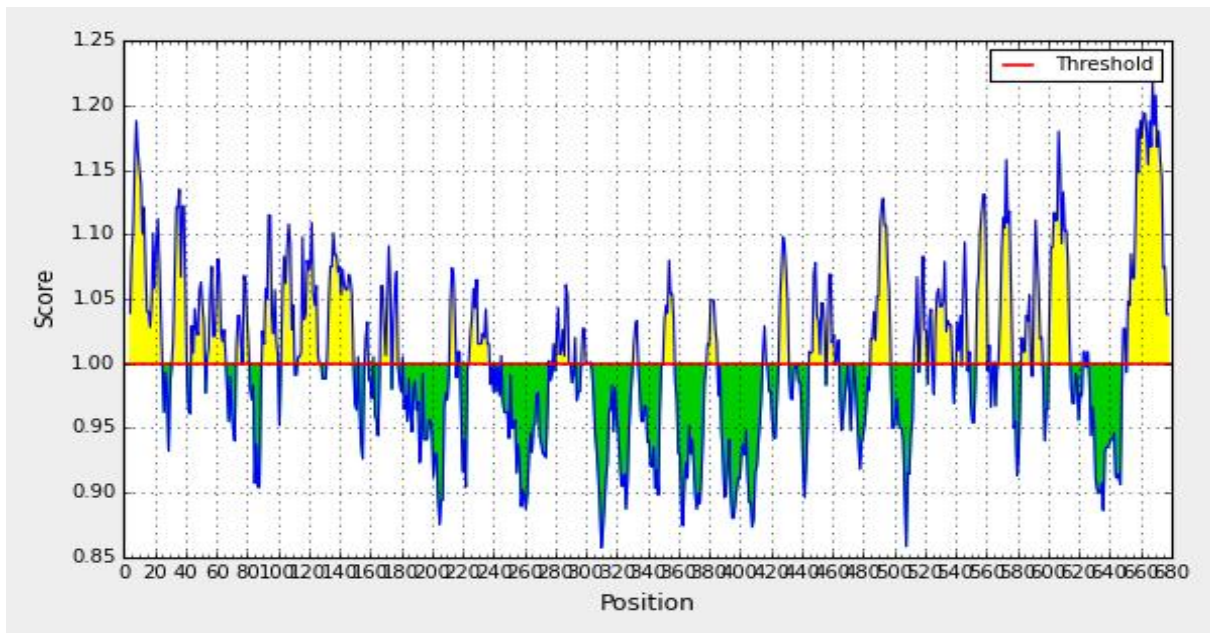


Figure 4. Kolaskar and Tongaonkar antigenicity prediction of the proposed epitope with a threshold value of 1.00. Residues in yellow regions are antigenic in nature.

Table 2. Predicted B-cell linear epitopes with ABCpred score, antigenicity score and hydrophilicity score.

Epitope	Position	ABCpred score	Antigenicity (IEDB)	Hydrophilicity (IEDB)
PLEASKRWAFRTGVPP	63-78	0.89	0.98	1.61
GKSLLLDPPTNVRDYP	102-117	0.69	1.05	1.27
LHLWGAFFLYDRIAST	137-152	0.86	1.06	1.44
ASTTMYRGKVFTEGNI	150-165	0.85	0.98	1.73

3.4. The T cell epitopes are bound and processed by MHC molecules

The 9-mer T cell epitopes were cross-referenced with MHC I processing and binding results. Only the epitopes with a total score (proteosomal processing, TAP transport, MHC binding) above 0.5 and an IC₅₀ < 250 nM were selected for further analysis (Table 2). Finally, only 5 epitopes were selected based on the criteria which interacted with several HLA alleles. Following this, T cell epitopes interacting with MHC II molecules were also identified based on MHC II binding results based on lower total percentile ranks and IC₅₀ < 500 nM. A total of 5 epitopes, which interacted with several HLA alleles, with similarities to the ones identified before were selected in this case (Table 3 and 4).

Table 3. Predicted epitopes for CD8+ T-cell along with their interacting MHC class I alleles with affinity < 250 nM.

Epitope	Position	MHC class I allele with total score having IC ₅₀ values < 250 nM
LEASKRWAF	64-72	HLA-B*18:01(1.05), HLA-B*15:03(.91), HLA-B*41:03(.57), HLA-B*41:04(.37), HLA-B*41:02(.32), HLA-B*44:02(.23), HLA-B*44:27(.23), HLA-B*44:08(.06)
LLLDPPTNV	105-113	HLA-A*02:11(1.09), HLA-A*02:03(.68), HLA-A*02:16(.65), HLA-A*02:50(.58), HLA-A*02:12(.58), HLA-A*02:01(.46), HLA-A*02:02(.38), HLA-A*02:19(.3), HLA-A*02:06(.2)
IALHLWGAF	135-143	HLA-B*15:03(1.23), HLA-B*15:17(.77), HLA-B*15:02(.47), HLA-B*35:01(.41), HLA-A*32:07(.21), HLA-B*15:01(.15)
HLWGAFFLY	138-146	HLA-A*29:02(1.88), HLA-A*80:01(1.35), HLA-B*15:03(.97), HLA-A*32:07(.59), HLA-A*68:23(.56), HLA-A*30:02(.52), HLA-A*32:01(.48), HLA-A*32:15(.28), HLA-B*35:01(.2), HLA-A*03:01(.19), HLA-A*03:02(.14)
TTMYRGKVF	152-160	HLA-B*15:17(1.32), HLA-B*15:03(.8), HLA-C*12:03(.73), HLA-A*26:02(.43), HLA-C*14:02(.08)

197
198

Table 4. Predicted CD4+ T-cell epitopes along with their interacting MHC class II alleles with affinity (IC50) < 500 nM and respective total scores.

Epitope	Position	MHC class II allele with percentile rank having IC50 values < 500 nM
DSPLEASKRWAFRTG	61-75	HLA-DRB1*03:01 (5.77), HLA-DRB1*09:01 (10.07), HLA-DRB3*01:01 (11.91), HLA-DRB1*07:01 (14.01), HLA-DRB1*15:01 (19.58)
GKSLLLDPPTNVRDY	102-116	HLA-DRB1*03:01 (0.25), HLA-DRB3*01:01 (1.5), HLA-DRB1*13:02 (2.3), HLA-DRB1*04:01 (3.26), HLA-DRB3*02:02 (6.5), HLA-DRB1*12:01 (12.6), HLA-DRB1*04:05 (14.63), HLA-DRB1*01:01 (18.99)
AQGIALHLWGAFFLY	132-146	HLA-DPA1*01:03/DPB1*02:01 (0.12), HLA-DQA1*01:01/DQB1*05:01 (1.96), HLA-DRB1*15:01 (2.42), HLA-DPA1*01/DPB1*04:01 (2.43), HLA-DPA1*02:01/DPB1*01:01 (5.21)
IALHLWGAFFLYDRI	135-149	HLA-DPA1*01/DPB1*04:01 (0.01), HLA-DPA1*01:03/DPB1*02:01 (0.02), HLA-DPA1*02:01/DPB1*01:01 (1.05), HLA-DQA1*01:01/DQB1*05:01 (1.24), HLA-DPA1*03:01/DPB1*04:02 (2.51), HLA-DRB1*15:01 (2.77), HLA-DPA1*02:01/DPB1*05:01 (4.67)
IASTTMYRGKVFTEG	149-163	HLA-DQA1*01:02/DQB1*06:02 (14.69), HLA-DRB1*15:01 (15.04), HLA-DPA1*01/DPB1*04:01 (17.46)

199

200

3.5. The candidate epitopes are highly conserved and cover large portions of the population

201

202

203

204

205

206

207

208

209

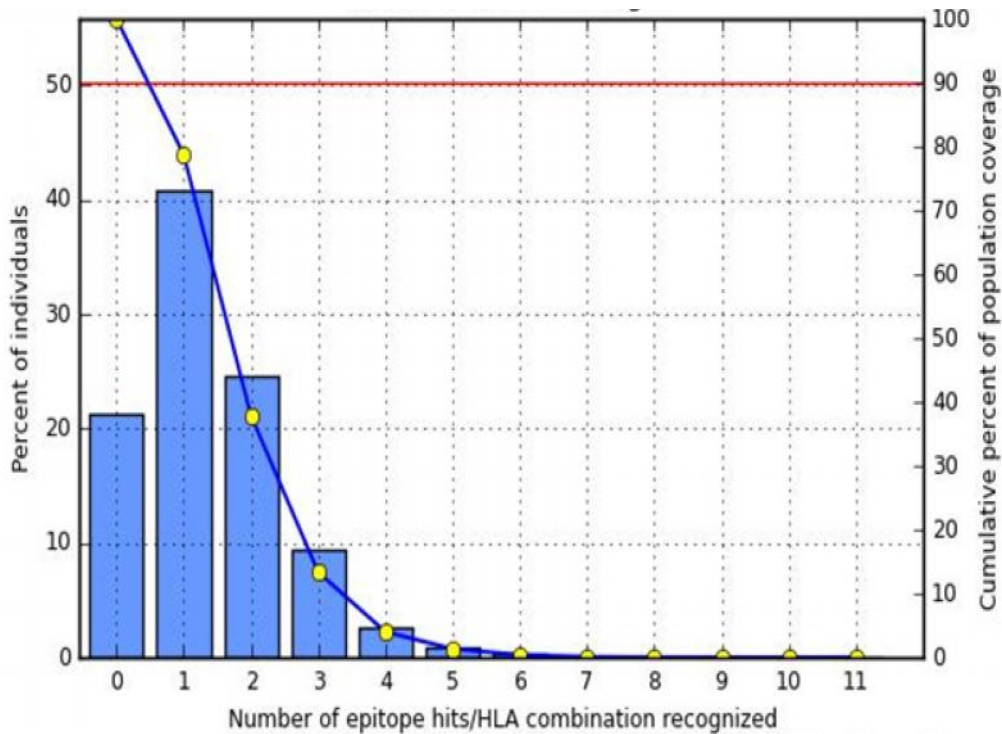
210

Selection of conserved epitopes confers broader protection against multiple strains, or even species, than epitopes selected from highly variable regions. Therefore, in an epitope based vaccine approach, an ideal epitope should be highly conserved. The epitopes identified in the previous assays were tested for conservancy using the IEDB resources. The epitopes "LEASKRWAF" and "DSPLEASKRWAFRTG" had 100% and 93.62% conservancy in the 47 glycoprotein (GP) sequences (Table 5). Population coverage analyses were also carried out for the epitopes, and it revealed that epitopes interacting with MHC class I molecules had a worldwide coverage of 78.74% (Figure 5.a). On the other hand, the epitopes interacting with MHC class II molecules had a worldwide coverage of 75.75% (Figure 5.b).

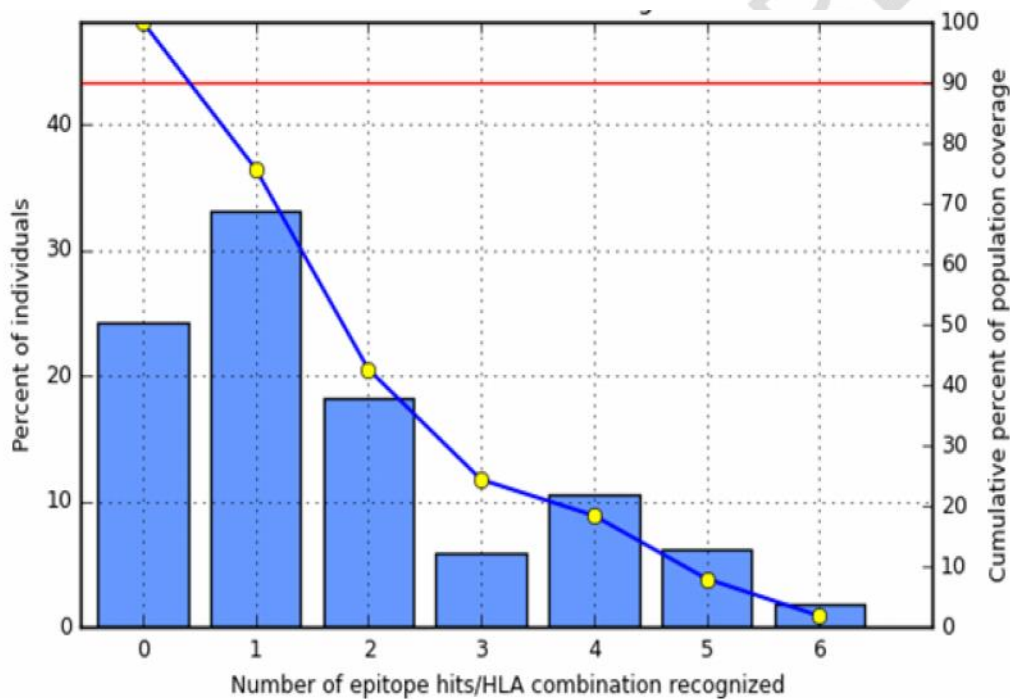
Table 5. Conservancy analysis of all the epitopes identified in the study.

Epitope sequence	Epitope length	Conservancy	Minimum identity	Maximum identity
HLWGAFFLY	9	100.00% (47/47)	100.00%	100.00%
TTMYRGKVF	9	80.85% (38/47)	88.89%	100.00%
IALHLWGAF	9	100.00% (47/47)	100.00%	100.00%
LLDPPTNV	9	55.32% (26/47)	77.78%	100.00%
LEASKRWAF	9	100.00% (47/47)	100.00%	100.00%
DSPLEASKRWAFRTG	15	93.62% (44/47)	93.33%	100.00%
GKSLLLDPPTNVRDY	15	55.32% (26/47)	86.67%	100.00%
AQGIALHLWGAFFLY	15	100.00% (47/47)	100.00%	100.00%
IALHLWGAFFLYDRI	15	82.98% (39/47)	93.33%	100.00%
IASTTMYRGKVFTEG	15	63.83% (30/47)	93.33%	100.00%

211



a.

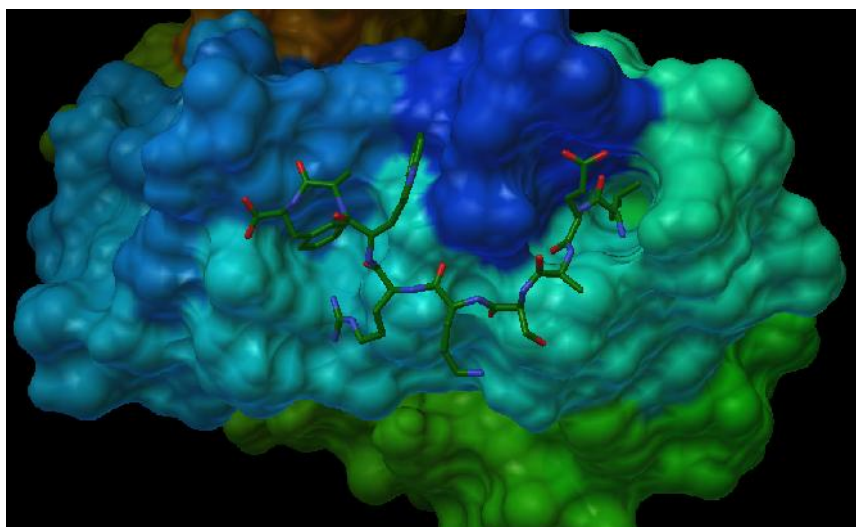


b.

Figure 5. Worldwide population coverage of epitopes with (a) MHC class I alleles and (b) MHC class II alleles respectively.

3.6. The T cell epitope and B cell epitope has high affinity for HLAs

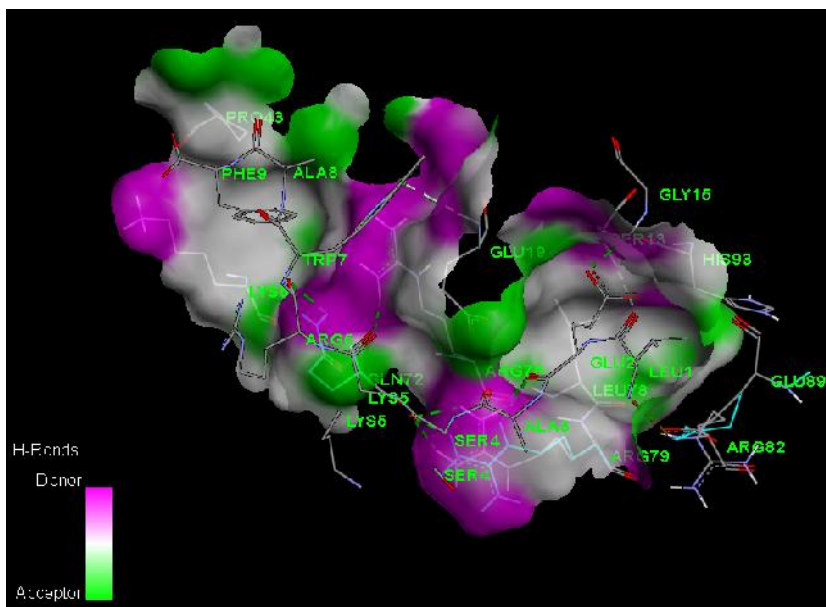
The T cell epitope "LEASKRWAF" interacted with MHC class I allele HLA-B*18:01 (PDB ID: 4XXC) at its binding pocket (Figure 6). This yielded binding affinity of -7.2 kcal/mol indicates a good interaction, while epitope "LLLDPPTNV" interacted with HLA-A*02:03 (PDB ID: 3OX8) with a binding affinity of -8.4 kcal/mol. On the other hand, epitope "DSPLEASKRWAFRTG" interacted with MHC class II allele HLA-DRB1*15:01 (PDB ID: 5V4M) yielded binding affinity of -6.9 kcal/mol (Figure 6). The epitope "GKSLLDPPTNVRDY", however, interacted with HLA-DRB1*04:01 (PDB ID: 5JLZ) with binding affinity of -6.6 kcal/mol.



227
228

a.

UNDER PEER REVIEW



230

231

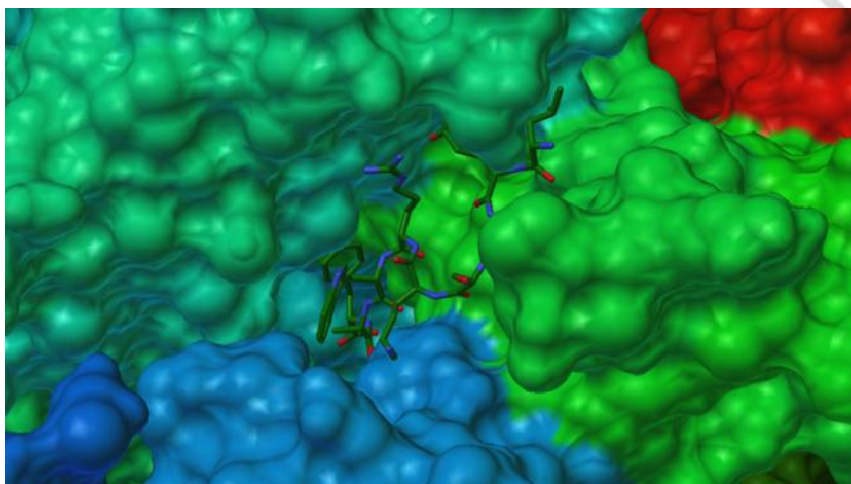
232

233

234

b.

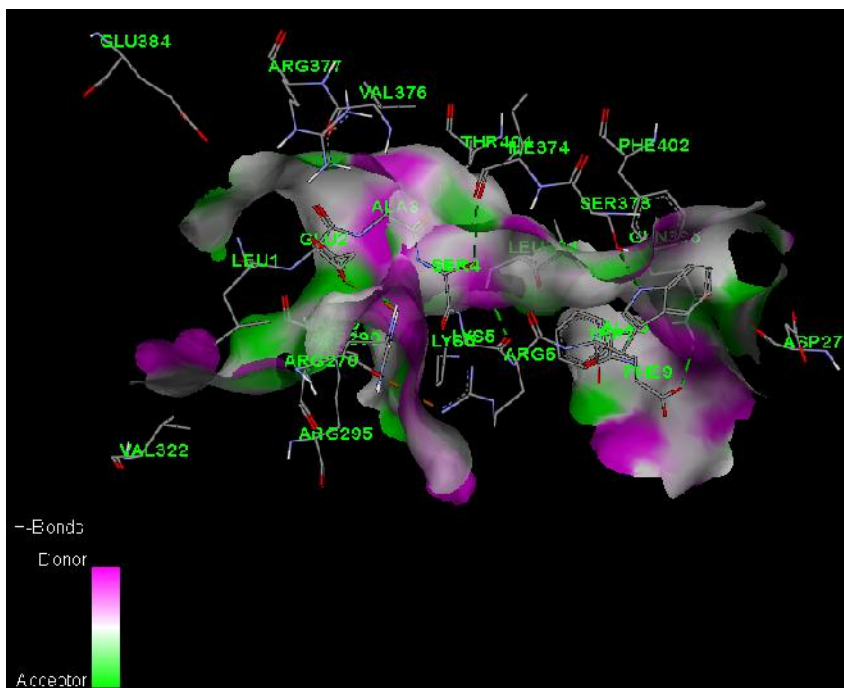
Figure 6. (a) Molecular docking of epitope “LEASKRWAF” with HLA-B*18:01 (PDB ID: 4XXC) yielded binding affinity = -7.2 kcal/mol; (b) H-bond receptor surface of HLA-B*18:01 depicting non-bond interactions.



235

236

a.



237
238 **b.**
239 **Figure 7.** (a) Molecular docking of epitope “DSPLEASKRWAFRTG” with HLA-DRB1*15:01 (PDB ID: 5V4M)
240 yielded binding affinity = -6.9 kcal/mol (b) H-bond receptor surface of HLA-DRB1*15:01 depicting non-bond
241 interactions.

242 3.7. The peptide vaccine candidates are non-toxic and do not cross the blood-brain barrier

244 The ADMET analysis results carried out with SwissADME tool and were cross-referenced with those of admetSAR server.
245 It was found that both of the peptide vaccine candidates could not cross the blood brain barrier, but they were readily
246 absorbed in the human intestine. These epitopes are non-inhibitors of P-glycoproteins, renal organic cation transporter,
247 and many of the CYP450 enzymes. They also have a low CYP inhibitory promiscuity and Non-AMES toxic and non-
248 carcinogens in nature (Table 6).

249
250 Table 6. ADMET assessment of epitope “LEASKRWAF” and “DSPLEASKRWAFRTG”.

Model	Result	Probability	Result	Probability
Absorption	“LEASKRWAF”		“DSPLEASKRWAFRTG”	
Blood-Brain Barrier	BBB-	0.8969	BBB-	0.9856
Human Intestinal Absorption	HIA+	0.8349	HIA+	0.8617
P-glycoprotein Inhibitor	Non-inhibitor	0.8835	Non-inhibitor	0.6331
Renal Organic Cation Transporter	Non-inhibitor	0.7958	Non-inhibitor	0.7665
Metabolism				
CYP450 1A2 Inhibitor	Non-inhibitor	0.821	Non-inhibitor	0.8043
CYP450 2C9 Inhibitor	Non-inhibitor	0.8141	Non-inhibitor	0.8002
CYP450 2D6 Inhibitor	Non-inhibitor	0.8809	Non-inhibitor	0.898
CYP450 3A4 Inhibitor	Non-inhibitor	0.7562	Inhibitor	0.5
CYP Inhibitory Promiscuity	Low CYP Inhibitory Promiscuity	0.9103	Low CYP Inhibitory Promiscuity	0.868
Toxicity				
AMES Toxicity	Non-AMES toxic	0.7156	Non-AMES toxic	0.7249
Carcinogens	Non-carcinogens	0.9137	Non-carcinogens	0.8413
Acute Oral Toxicity	III	0.5991	III	0.5795

3.8. The in vivo results verify the in-silico workflow

The results of the study remained questionable until it was tested and found to be concordant with in vivo results. The negative control or random sequence failed to pass through the steps of the workflow. On the contrary, four of the six peptides tested by Shi et al. [61] were identified as antigenic epitopes in our workflow as well. However, PEP37 and PEP71 were filtered out in our workflow. Random sequence used as negative control failed to pass the first step of the workflow.

In this study, we focused on designing epitope based universal vaccine with global efficacy against these two deadly viruses. For that, we selected the glycoprotein (GP) out of seven different proteins produced by both viruses as it contains large conserved region positioned on the outer membrane that may easily facilitate to mount immune response. From the epitope conservancy analysis, the two epitopes "LEASKRWAF" (64 a.a-72 a.a.) and "DSPLEASKRWAFRTG" (61 a.a.-75 a.a) have been found 100% and 93.62% conserved in the 47 GP sequences respectively and population coverage analysis revealed that epitopes "LEASKRWAF" interacting with MHC class I molecules and "DSPLEASKRWAFRTG" interacting with MHC class II molecules had worldwide coverage of 78.74% and 75.75% respectively. As the high epitope conservancy and large population coverage are the prerequisites of vaccine candidate, the both peptides fulfill these criteria. ABCpred and IEDB software identified the B cell epitope "PLEASKRWAFRTGVPP" (63 a.a-78 a.a) which has higher surface accessibility scores, hydrophilicity scores and antigenicity scores that are the crucial requirements of an epitope to be considered as vaccine. Most importantly, B cell and T cell epitope have sequence similarity which indicates that same epitope can induce both B cell and T cell mediated immunity. From the molecular docking analysis, it was found that the binding affinity of "LEASKRWAF" epitope interacted with MHC class I allele HLA-B*18:01 was -7.2 kcal/mol and "DSPLEASKRWAFRTG" interacted with MHC class II allele HLA-DRB1*15:01 was -6.9 kcal/mol, which indicates good interaction between epitope and allele. The ADMET analysis revealed that both peptide vaccine candidates were not susceptible to cross the blood brain barrier, non-AMES toxic and non-carcinogens in nature. Finally, the epitopes were category III oral toxic compounds, but the dosage needed to cause toxicity is very high (500-5000 mg/kg), and therefore poses minimal risk.

Most vaccine currently available is based on either inactivated or live-attenuated pathogen, but the major drawback of these vaccines is the safety issue as they may reactivate in the human body and cause deleterious effect. In this case, epitope based vaccine can mitigate or avoid the possible harmful effects as it contains only a short peptide. Currently vaccine development using bioinformatics has gained popularity as it reduces time consuming trial and error process and can be exploited to develop vaccine against emerging viruses within a very short time. In a previous study, Raju Das et al. [65] designed an epitope based vaccine against Ebola virus and in another study, Anum Munir et al. [66] proposed another epitope based peptide vaccine against Marburg virus. But to our best knowledge till now, there is no combined single vaccine design against these two deadly viruses.

5. CONCLUSION

This study suggests two potential epitopes to design epitope-based universal vaccine for all Ebola and Marburg viruses. Our results are based on sequence data analysis of surface glycoprotein and binding interaction between MHC molecules. Both in vitro and in vivo experiments are needed for justifying their ability to elicit the immune response against these deadly viruses.

COMPETING INTERESTS

The authors declare that they have no conflict of interest.

REFERENCES

1. Yang XL, Tan CW, Anderson DE, et al. Characterization of a filovirus (Mengla virus) from Rousettus bats in China. *Nature microbiology*. 2019.
2. Reynolds P, Marzi A. Ebola and Marburg virus vaccines. *Virus genes*. 2017;53(4):501-515.
3. Brainard J, Hooper L, Pond K, Edmunds K, Hunter PR. Risk factors for transmission of Ebola or Marburg virus disease: a systematic review and meta-analysis. *International journal of epidemiology*. 2016;45(1):102-116.
4. Gordon TB, Hayward JA, Marsh GA, Baker ML, Tachedjian G. Host and Viral Proteins Modulating Ebola and Marburg Virus Egress. *Viruses*. 2019;11(1).
5. Towner JS, Amman BR, Sealy TK, et al. Isolation of Genetically Diverse Marburg Viruses from Egyptian Fruit Bats. *PLoS Pathogens*. 2009;5(7):e1000536.

- 309 6. Goldstein T, Anthony SJ, Gbakima A, et al. The discovery of Bombali virus adds further support for bats as hosts
310 of ebolaviruses. *Nature microbiology*. 2018;3(10):1084-1089.
- 311 7. Feldmann H, Klenk HD, Sanchez A. Molecular biology and evolution of filoviruses. *Archives of virology*.
312 Supplementum. 1993;7:81-100.
- 313 8. Brainard J, Pond K, Hooper L, Edmunds K, Hunter P. Presence and Persistence of Ebola or Marburg Virus in
314 Patients and Survivors: A Rapid Systematic Review. *PLoS neglected tropical diseases*. 2016;10(2):e0004475.
- 315 9. Taylor DJ, Leach RW, Bruenn J. Filoviruses are ancient and integrated into mammalian genomes. *BMC*
316 *Evolutionary Biology*. 2010;10:193-193.
- 317 10. Martin B, Hoenen T, Canard B, Decroly E. Filovirus proteins for antiviral drug discovery: A structure/function
318 analysis of surface glycoproteins and virus entry. *Antiviral research*. 2016;135:1-14.
- 319 11. Xu W, Edwards MR, Borek DM, et al. Ebola virus VP24 targets a unique NLS binding site on karyopherin alpha 5
320 to selectively compete with nuclear import of phosphorylated STAT1. *Cell host & microbe*. 2014;16(2):187-200.
- 321 12. Valmas C, Grosch MN, Schumann M, et al. Marburg virus evades interferon responses by a mechanism distinct
322 from ebola virus. *PLoS pathogens*. 2010;6(1):e1000721.
- 323 13. Ramanan P, Edwards MR, Shabman RS, et al. Structural basis for Marburg virus VP35-mediated immune
324 evasion mechanisms. *Proceedings of the National Academy of Sciences of the United States of America*.
325 2012;109(50):20661-20666.
- 326 14. Albarino CG, Shoemaker T, Khristova ML, et al. Genomic analysis of filoviruses associated with four viral
327 hemorrhagic fever outbreaks in Uganda and the Democratic Republic of the Congo in 2012. *Virology*.
328 2013;442(2):97-100.
- 329 15. Babirye P, Musubika C, Kirimunda S, et al. Identity and validity of conserved B cell epitopes of filovirus
330 glycoprotein: towards rapid diagnostic testing for Ebola and possibly Marburg virus disease. *BMC infectious*
331 *diseases*. 2018;18(1):498.
- 332 16. Lee JE, Fusco ML, Hessel AJ, Oswald WB, Burton DR, Saphire EO. Structure of the Ebola virus glycoprotein
333 bound to an antibody from a human survivor. *Nature*. 2008;454(7201):177-182.
- 334 17. Klenk H-D, Feldmann H. Ebola and Marburg viruses: molecular and cellular biology. Garland Science; 2004.
- 335 18. Shabman RS, Jabado OJ, Mire CE, et al. Deep sequencing identifies noncanonical editing of Ebola and Marburg
336 virus RNAs in infected cells. *mBio*. 2014;5(6):e02011.
- 337 19. Côté M, Misasi J, Ren T, et al. Small molecule inhibitors reveal Niemann-Pick C1 is essential for ebolavirus
338 infection. *Nature*. 2011;477(7364):344-348.
- 339 20. Marzi A, Engelmann F, Feldmann F, et al. Antibodies are necessary for rVSV/ZEBOV-GP-mediated protection
340 against lethal Ebola virus challenge in nonhuman primates. *Proceedings of the National Academy of Sciences of*
341 *the United States of America*. 2013;110(5):1893-1898.
- 342 21. Geisbert TW. First Ebola virus vaccine to protect human beings? *Lancet (London, England)*.
343 2017;389(10068):479-480.
- 344 22. Keusch G, McAdam K, Cuff P, Mancher M, Busta E. Integrating clinical research into epidemic response: the
345 Ebola experience. *Integrating clinical research into epidemic response: the Ebola experience*. 2017.
- 346 23. Corti D, Misasi J, Mulangu S, et al. Protective monotherapy against lethal Ebola virus infection by a potently
347 neutralizing antibody. *Science*. 2016;351(6279):1339-1342.
- 348 24. Mire CE, Geisbert JB, Borisevich V, et al. Therapeutic treatment of Marburg and Ravn virus infection in
349 nonhuman primates with a human monoclonal antibody. *Science translational medicine*. 2017;9(384).
- 350 25. Pascal KE, Dudgeon D, Trefry JC, et al. Development of Clinical-Stage Human Monoclonal Antibodies That Treat
351 Advanced Ebola Virus Disease in Nonhuman Primates. *The Journal of infectious diseases*.
352 2018;218(suppl_5):S612-S626.
- 353 26. Qiu X, Fernando L, Melito PL, et al. Ebola GP-specific monoclonal antibodies protect mice and guinea pigs from
354 lethal Ebola virus infection. *PLoS neglected tropical diseases*. 2012;6(3):e1575.
- 355 27. Qiu X, Wong G, Audet J, et al. Reversion of advanced Ebola virus disease in nonhuman primates with ZMapp.
356 *Nature*. 2014;514(7520):47-53.
- 357 28. Qiu X, Audet J, Lv M, et al. Two-mAb cocktail protects macaques against the Makona variant of Ebola virus.
358 *Science translational medicine*. 2016;8(329):329ra333.
- 359 29. Davey RT, Jr., Dodd L, Proschan MA, et al. A Randomized, Controlled Trial of ZMapp for Ebola Virus Infection.
360 *The New England journal of medicine*. 2016;375(15):1448-1456.
- 361 30. Sivapalasingam S, Kamal M, Slim R, et al. Safety, pharmacokinetics, and immunogenicity of a co-formulated
362 cocktail of three human monoclonal antibodies targeting Ebola virus glycoprotein in healthy adults: a randomised,
363 first-in-human phase 1 study. *The Lancet. Infectious diseases*. 2018;18(8):884-893.
- 364 31. Wec AZ, Bornholdt ZA, He S, et al. Development of a Human Antibody Cocktail that Deploys Multiple Functions to
365 Confer Pan-Ebolavirus Protection. *Cell host & microbe*. 2019;25(1):39-48 e35.
- 366 32. Bornholdt ZA, Herbert AS, Mire CE, et al. A Two-Antibody Pan-Ebolavirus Cocktail Confers Broad Therapeutic
367 Protection in Ferrets and Nonhuman Primates. *Cell host & microbe*. 2019;25(1):49-58 e45.

- 368 33. Brannan JM, He S, Howell KA, et al. Post-exposure immunotherapy for two ebolaviruses and Marburg virus in
369 nonhuman primates. *Nature communications*. 2019;10(1):105.
- 370 34. Rahim MN, Wee EG, He S, et al. Complete protection of the BALB/c and C57BL/6J mice against Ebola and
371 Marburg virus lethal challenges by pan-filovirus T-cell epitope vaccine. *PLoS pathogens*. 2019;15(2):e1007564.
- 372 35. Edgar RC. MUSCLE: multiple sequence alignment with high accuracy and high throughput. *Nucleic Acids
373 Research*. 2004;32(5):1792-1797.
- 374 36. Kumar S, Stecher G, Tamura K. MEGA7: Molecular Evolutionary Genetics Analysis Version 7.0 for Bigger
375 Datasets. *Molecular biology and evolution*. 2016;33(7):1870-1874.
- 376 37. Waterhouse AM, Procter JB, Martin DM, Clamp M, Barton GJ. Jalview Version 2--a multiple sequence alignment
377 editor and analysis workbench. *Bioinformatics (Oxford, England)*. 2009;25(9):1189-1191.
- 378 38. Garcia-Boronat M, Diez-Rivero CM, Reinherz EL, Reche PA. PVS: a web server for protein sequence variability
379 analysis tuned to facilitate conserved epitope discovery. *Nucleic acids research*. 2008;36(Web Server
380 issue):W35-41.
- 381 39. Krogh A, Larsson B, von Heijne G, Sonnhammer EL. Predicting transmembrane protein topology with a hidden
382 Markov model: application to complete genomes. *Journal of molecular biology*. 2001;305(3):567-580.
- 383 40. Hansen JE, Lund O, Tolstrup N, Gooley AA, Williams KL, Brunak S. NetOglyc: prediction of mucin type O-
384 glycosylation sites based on sequence context and surface accessibility. *Glycoconjugate journal*. 1998;15(2):115-
385 130.
- 386 41. Chuang G-Y, Boyington JC, Joyce MG, et al. Computational prediction of N-linked glycosylation incorporating
387 structural properties and patterns. *Bioinformatics (Oxford, England)*. 2012;28(17):2249-2255.
- 388 42. Doytchinova IA, Flower DR. VaxiJen: a server for prediction of protective antigens, tumour antigens and subunit
389 vaccines. *BMC bioinformatics*. 2007;8:4.
- 390 43. Bui HH, Sidney J, Li W, Fusseder N, Sette A. Development of an epitope conservancy analysis tool to facilitate
391 the design of epitope-based diagnostics and vaccines. *BMC Bioinformatics*. 2007;8:361.
- 392 44. Jespersen MC, Peters B, Nielsen M, Marcatili P. BepiPred-2.0: improving sequence-based B-cell epitope
393 prediction using conformational epitopes. *Nucleic Acids Research*. 2017;45.
- 394 45. Chen H, Gu F, Huang Z. Improved Chou-Fasman method for protein secondary structure prediction. *BMC
395 Bioinformatics*. 2006;7(Suppl 4):S14-S14.
- 396 46. Kolaskar AS, Tongaonkar PC. A semi-empirical method for prediction of antigenic determinants on protein
397 antigens. *FEBS letters*. 1990;276(1-2):172-174.
- 398 47. Parker JM, Guo D, Hodges RS. New hydrophilicity scale derived from high-performance liquid chromatography
399 peptide retention data: correlation of predicted surface residues with antigenicity and X-ray-derived accessible
400 sites. *Biochemistry*. 1986;25(19):5425-5432.
- 401 48. Saha S, Raghava GP. Prediction of continuous B-cell epitopes in an antigen using recurrent neural network.
402 *Proteins*. 2006;65(1):40-48.
- 403 49. Bui HH, Sidney J, Dinh K, Southwood S, Newman MJ, Sette A. Predicting population coverage of T-cell epitope-
404 based diagnostics and vaccines. *BMC Bioinformatics*. 2006;7:153.
- 405 50. Vita R, Overton JA, Greenbaum JA, et al. The immune epitope database (IEDB) 3.0. *Nucleic Acids Res*.
406 2015;43(Database issue):D405-412.
- 407 51. Fleri W, Paul S, Dhanda SK, et al. The Immune Epitope Database and Analysis Resource in Epitope Discovery
408 and Synthetic Vaccine Design. *Frontiers in Immunology*. 2017;8:278.
- 409 52. Zhang Q, Wang P, Kim Y, et al. Immune epitope database analysis resource (IEDB-AR). *Nucleic Acids Research*.
410 2008;36(Web Server issue):W513-W518.
- 411 53. Agatonovic-Kustrin S, Beresford R. Basic concepts of artificial neural network (ANN) modeling and its application
412 in pharmaceutical research. *Journal of pharmaceutical and biomedical analysis*. 2000;22(5):717-727.
- 413 54. Bhasin M, Raghava GP. Prediction of CTL epitopes using QM, SVM and ANN techniques. *Vaccine*. 2004;22(23-
414 24):3195-3204.
- 415 55. Nielsen M, Lundegaard C, Lund O. Prediction of MHC class II binding affinity using SMM-align, a novel
416 stabilization matrix alignment method. *BMC Bioinformatics*. 2007;8:238-238.
- 417 56. Lamiable A, Thevenet P, Rey J, Vavrusa M, Derreumaux P, Tuffery P. PEP-FOLD3: faster de novo structure
418 prediction for linear peptides in solution and in complex. *Nucleic Acids Res*. 2016;44(W1):W449-454.
- 419 57. Trott O, Olson AJ. AutoDock Vina: improving the speed and accuracy of docking with a new scoring function,
420 efficient optimization and multithreading. *Journal of computational chemistry*. 2010;31(2):455-461.
- 421 58. Kimmish H, Fasnacht M, Yan L. Fully automated antibody structure prediction using BIOVIA tools: Validation
422 study. *PLoS ONE*. 2017;12(5):e0177923.
- 423 59. Daina A, Michielin O, Zoete V. SwissADME: a free web tool to evaluate pharmacokinetics, drug-likeness and
424 medicinal chemistry friendliness of small molecules. *Scientific Reports*. 2017;7:42717.
- 425 60. Cheng F, Li W, Zhou Y, et al. admetSAR: a comprehensive source and free tool for assessment of chemical
426 ADMET properties. *Journal of chemical information and modeling*. 2012;52(11):3099-3105.

- 427 **61.** Shi J, Feng H, Lee J, Ning Chen W. Comparative proteomics profile of lipid-cumulatg oleaginous yeast: an
428 iTRAQ-coupled 2-D LC-MS/MS analysis. PloS one. 2013;8(12):e85532.
- 429 **62.** Blythe MJ, Flower DR. Benchmarking B cell epitope prediction: underperformance of existing methods. Protein
430 science : a publication of the Protein Society. 2005;14(1):246-248.
- 431 **63.** Yang X, Yu X. An introduction to epitope prediction methods and software. Reviews in medical virology.
432 2009;19(2):77-96.
- 433 **64.** Gao J, Faraggi E, Zhou Y, Ruan J, Kurgan L. BEST: Improved Prediction of B-Cell Epitopes from Antigen
434 Sequences. PloS one. 2012;7(6):e40104.
- 435 **65.** Dash R, Das R, Junaid M, Akash MF, Islam A, Hosen SZ. In silico-based vaccine design against Ebola virus
436 glycoprotein. Adv Appl Bioinform Chem. 2017;10:11-28.
- 437 **66.** Munir A, Maria M, Mehmood A, Shah M, Fazal S. In-silico epitopebased vaccine an excellent solution against
438 Marburg virus. Journal of Innovations in Pharmaceutical and Biological Sciences(JIPBS). 2016;3(4).
439

440
441

UNDER PEER REVIEW